

# Improvement of the critical speed in high-speed ballasted railway tracks with stone columns: A numerical study on critical length

Jesús Fernández-Ruiz<sup>a,\*</sup>, Marina Miranda<sup>b</sup>, Jorge Castro<sup>b</sup>, Luis Medina Rodríguez<sup>a</sup>

<sup>a</sup> University of La Coruña, Department of Civil Engineering, Campus de Elviña, 15071 La Coruña, Spain

<sup>b</sup> University of Cantabria, Department of Ground Engineering and Materials Science, Avda. Castros 44, 39005 Santander, Spain

## ARTICLE INFO

### Keywords:

Stone columns  
Critical length  
Critical speed  
High-speed railway lines  
3D dynamic numerical model

## ABSTRACT

The pressure to achieve a higher speed of train operation has increased in the last few years due to the development of high-speed railway lines. In the presence of soft soils, this speed increase is not possible without undertaking soil improvement measures, since the critical speed is lower than the desired speed of train operation. One of the most widely used soil improvement techniques is that of stone columns. In relation to these is the concept of critical length which, up to now, has only been studied for static cases. This research focuses, for the first time, on the enhancement of the critical speed in high-speed railways with stone columns and with special reference to critical length. Moreover, others parameters such as: maximum rail displacement and Dynamic Amplification Factor (DAF) are also studied. Analysing three profiles of ground representative of soft soils, it can be observed how the effect of the stone columns on critical speed is relevant, showing that critical length is different with respect to the three parameters above, the most restrictive one being that which corresponds to the critical speed. The influence of other parameters on the critical length and on the effectiveness of stone columns, such as the area replacement ratio, the dynamic pressure bulb and the existing soil stiffness is analysed and discussed.

## Introduction

The development of the railway is rapidly gathering pace, with constant demands for faster and heavier vehicles. This continuous increase in speed of train operation places increasingly greater demands on the track-ground system from a geotechnical point of view. The relationship between displacements on the track and train speed has been studied (e.g., [45]) and the speed at which the rail displacement is maximum is known as the “critical speed”, which occurs when the speed of the train equals or exceeds the speed of wave propagation in the track-ground system. This phenomenon is associated with a considerable increase in ground strains, which may even be permanent (e.g., [39,5]). The phenomenon acquires a very important dimension in high-speed lines (e.g., [35,31]) and can be critical in the case of soft soils.

Formally, the critical speed is the speed of a non-oscillating moving load that implies the greatest amplification of the dynamic response, being completely determined by the properties of wave propagation in the embankment-foundation soil system and by the bending wave propagation in the track (e.g., [15,16,41,4]). This important topic, critical speed, has been widely studied in recent years and it can be said

that the phenomenon is now well understood [4]. The origins of this area of study are to be found in the 1990 s when the Ledsgard case marked the beginnings of the experimental and numerical study of the critical speed phenomenon on soft soils [38,31,27,44,30,2].

When a new line is built or an existing line requires an increase in the speed of train operation, it is fundamental, from the geotechnical viewpoint, to study the stiffness of the underlying soil and there are three possible scenarios[17]:

1. Soil sufficiently stiff, on which the train speed is < 50% of the critical speed. No corrective measures are required
2. Soil with medium stiffness, on which the train speed is between 50 and 70% of the critical speed. It is not clear whether corrective measures are required
3. Soil with low stiffness, on which the train speed is greater than 70% of the critical speed. Corrective measures are required

When corrective measures are required, these can be of various types, the most important being soil replacement and soil improvement (e.g., [43,17]). One of the most widely used soil improvement techniques in geotechnical engineering practise is that of stone columns (e.

\* Corresponding author.

E-mail address: [jesus.fernandez.ruiz@udc.es](mailto:jesus.fernandez.ruiz@udc.es) (J. Fernández-Ruiz).

Nomenclature			
$a_r$	Area replacement ratio: $a_r = A_c/A_T$	$L$	Column length
$A_c$	Column cross-sectional area	$L_{cr}$	Critical column length
$A_T$	Corresponding area improved by stone columns	$L_{min}$	Distance between two adjacent loading nodes
$v$	Train (load) speed	$L_{db}$	Depth of dynamic pressure bulb
$v_{cr}$	Critical speed	$L_{sb}$	Depth of static pressure bulb
$B$	Width of loaded zone	VIF	Critical speed improvement factor: $VIF = v_{cr, reinf} / v_{cr, no reinf}$
$C_n$	Courant number	$\alpha, \beta$	Rayleigh damping coefficients
DAF	Dynamic Amplification Factor	$\Delta\sigma_c$	Increase in vertical stress in the column
$E$	Young's modulus	$\Delta\sigma_s$	Increase in vertical stress in the soil
$H$	Soft soil layer thickness	$\Delta t$	Dynamic time step
		$\gamma$	Specific weight
		$\nu$	Poisson's ratio

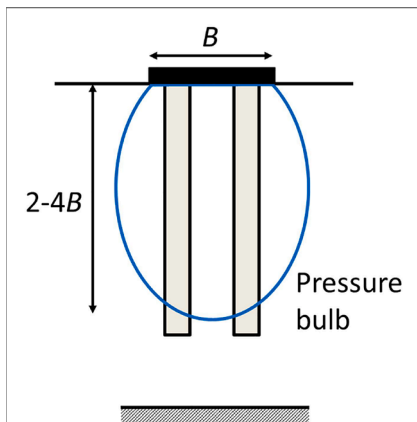


Fig. 1. Justification of critical column length in a homogeneous soil layer for settlement reduction in elastic materials [11].

g., [8,33,28]) which are vertical boreholes in the ground, filled upwards with gravel compacted by means of a vibrator. A key parameter of this soil improvement technique is the area replacement ratio, which is the ratio between column area and improved soil area ( $a_r = A_c/A_T$ ). Stone columns can reach a rigid stratum (end-bearing columns) or can be embedded in a soft soil (floating columns). In this latter case, the length of the stone columns is an important aspect of design with great economic repercussions. Soil replacement and soil improvement techniques require the economic optimisation of the solution adopted. Closely linked to soil improvement techniques is the concept of critical length, initially devised for piles, but of a similar importance for stone columns. Several authors have undertaken studies on this important concept [29,7,10] among others. Castro [11] found that the critical length of stone columns for settlement reduction is closely related to the extension of the pressure bulb below the foundation. The pressure bulb is a very useful concept, although strictly speaking it is only valid for elastic behaviour (Fig. 1).

The research carried out up to the present on the critical length of stone columns has focused on static loads [12]. To the authors'

knowledge, there are no specific studies of the concept of the critical length of stone columns (or of any other soil improvement technique) for dynamic loads and, of course, not for moving loads such as those related to railways. Moreover, there are no specific studies on the effectiveness of stone columns to enhance critical speed in high-speed railways. These facts, together with the existing uncertainty regarding criteria or specific studies on the depth of reinforcement of soft soils under high-speed railway tracks, are the main motivation for this paper, in which the first systematic and numerical study is made of the critical length of stone columns under high-speed ballasted tracks. Thus, this is considered to be the first study on the effectiveness of stone columns to improve critical speed in high-speed railway lines, with special emphasis in the critical length.

For this type of study, numerical models are suitable since they allow a systematic parametric analysis of a wide range of both ground and geometric conditions. Hence, to this end, a dynamic 3D numerical model of finite elements formulated in the time domain has been used, developed using the Plaxis software (Bringreave et al, 2019). This type of model has been applied to the study of railway critical speed [27,19,1,42,13] among others. Previously, the authors have validated this model both experimentally with real measurements [21,24] and numerically when comparing this model with a 2.5D FEM-BEM model formulated in the frequency and wavenumber domain [21]. Moreover, the authors have used this type of 3D numerical model for the study of vibrations induced by rail traffic [20,22,23]. For this type of soil reinforcement techniques, i.e. periodic arrays of columnar inclusions, a pure 3D model is required, although very recently periodic models have been developed [26] whose use is limited to academia.

The paper is organised according to the following schema i) the characteristics of the track and the ground are exposed, studying 3 different cases of soils for the same ballasted track; ii) the numerical model used is briefly outlined, highlighting its main characteristics; iii) the results obtained in the 3 cases studied without stone columns are presented, showing rail displacement vs. velocity for a single moving load; iv) the effect of the stone columns is analysed for the 3 cases studied and considering two replacement rates for each case. Specifically, the effects of the columns on the rail displacement, on the Dynamic Amplification Factor (DAF) and on the critical speed are studied, varying the depth of the stone columns; v) the results obtained from the

Table 1  
Soil and stone column dynamic properties.

	Layer depth (m)	Specific weight (kN/m <sup>3</sup> )	Young's modulus (MPa)	Poisson's ratio	Rayleigh Damping	
					$\alpha$ (s <sup>-1</sup> )	$\beta$ (s)
Homogeneous soil	0-∞	14.75	15.90	0.49	1.58	0.67·10 <sup>-3</sup>
Non-homogeneous soil 1	0-2	14.75	11.90	0.49	1.58	0.67·10 <sup>-3</sup>
	2-∞	14.75	11.90 + 2·(z-2)	0.49	1.58	0.67·10 <sup>-3</sup>
Non-homogeneous soil 2	0-2	14.75	32.00	0.49	1.58	0.67·10 <sup>-3</sup>
	2-∞	14.75	32.00 + 5.40·(z-2)	0.49	1.58	0.67·10 <sup>-3</sup>
Stone column	Variable	18.00	432.00	0.20	2.38	1.00·10 <sup>-3</sup>

**Table 2**  
Track properties.

	Layer thickness (m)	Specific weight (kN/m <sup>3</sup> )	Young's modulus (MPa)	Poisson's ratio	Rayleigh Damping	
					$\alpha$ (s <sup>-1</sup> )	$\beta$ (s)
Sleeper	0.22	25.00	30.00·10 <sup>3</sup>	0.20	0.39	0.16·10 <sup>-3</sup>
Ballast	0.35	16.00	97.00	0.12	2.38	1.00·10 <sup>-3</sup>
Subballast	0.55	19.00	212.00	0.20	1.58	0.67·10 <sup>-3</sup>

cases studied are discussed and compared; and, finally, vi) a series of interesting conclusions are provided for the design and calculation of stone columns in high-speed ballasted railways on soft soils.

**Numerical models**

*Geodynamic and track characteristics*

For the numerical study of the critical length of stone columns under high-speed railways, three ideal cases with only one soil layer have been studied, each one with different geotechnical properties of the foundation layer. These are shown in Table 1 together with the properties of the stone columns. As can be observed, the first case consists of a homogeneous soil and the other two are non-homogenous soils, because their stiffness increase with depth.

Ideal cases of only one soil layer have been considered to facilitate the analysis and interpretation of the results, although the geotechnical properties of the homogeneous soil have been taken based on those of

one of the existing soils in the Ledsgard case, specifically a Marine Clay. Its properties have been considered according to Alves Costa et al. [2] in which this soil is named as Clay 1. The S-wave propagation speed is equal to 60 m/s (216 km/h) for it. This soil has been considered because in the Ledsgard case the critical speed was approximately equal to 60 m/s (216 km/h) and it was intended to begin this study with the case of a homogeneous soil, since the results of this kind of soil are easier to interpret. Although from a geotechnical point of view this soil is very soft, it has been considered appropriate to include it as the initial soil of this study since it corresponds to an extreme case.

The critical speed in inversely dispersive soil profiles (i.e., those whose stiffness decreases with depth) is closely related to properties of the softer underlying layer (e.g., [4]). Therefore, in this case of homogeneous soil, it is to be expected that when the soil is reinforced in a finite length by stone columns, the critical speed will not be significantly affected and according to Alves Costa et al. [4] it should be between the S-wave propagation speed and that of the Rayleigh waves of the softer underlying layer. However, the authors think that this case is worth

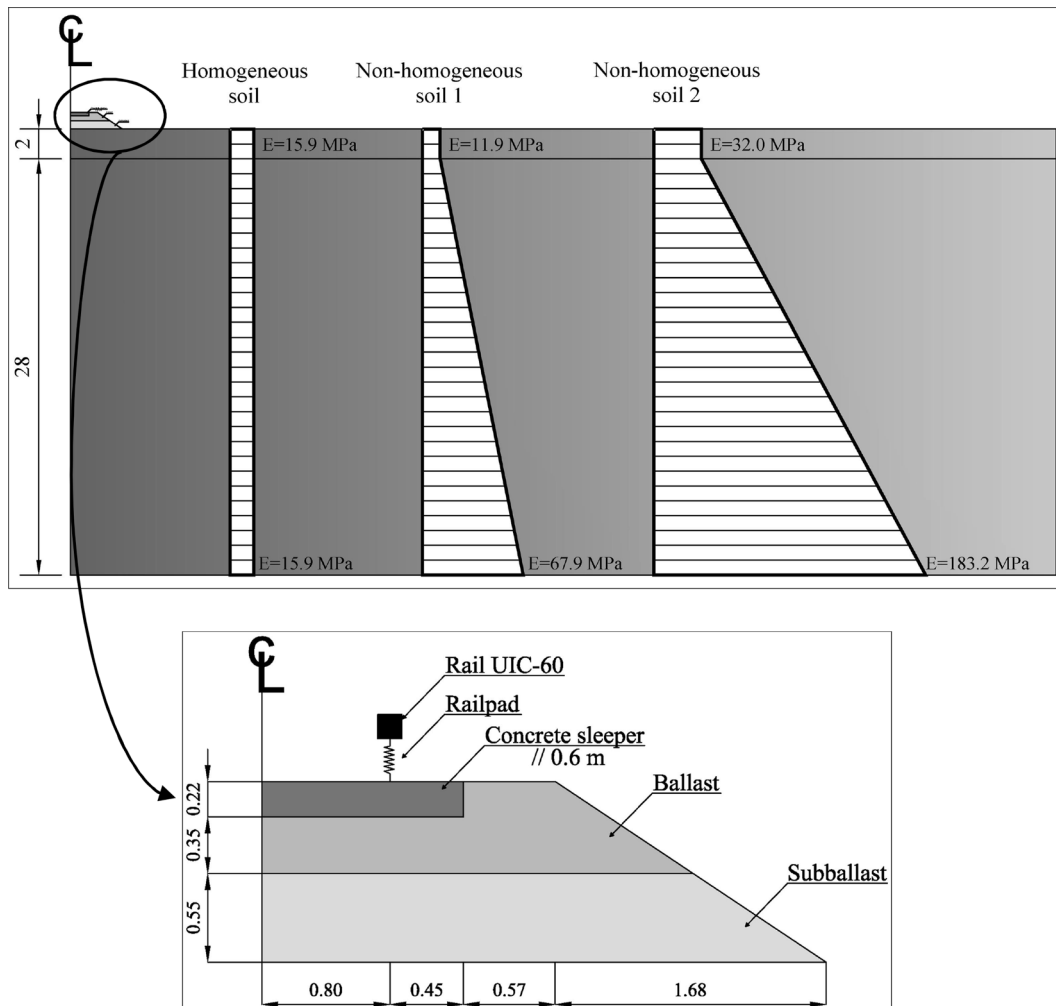


**Fig. 2.** Schematic representation of soil stiffness and railway track (distances in meters).

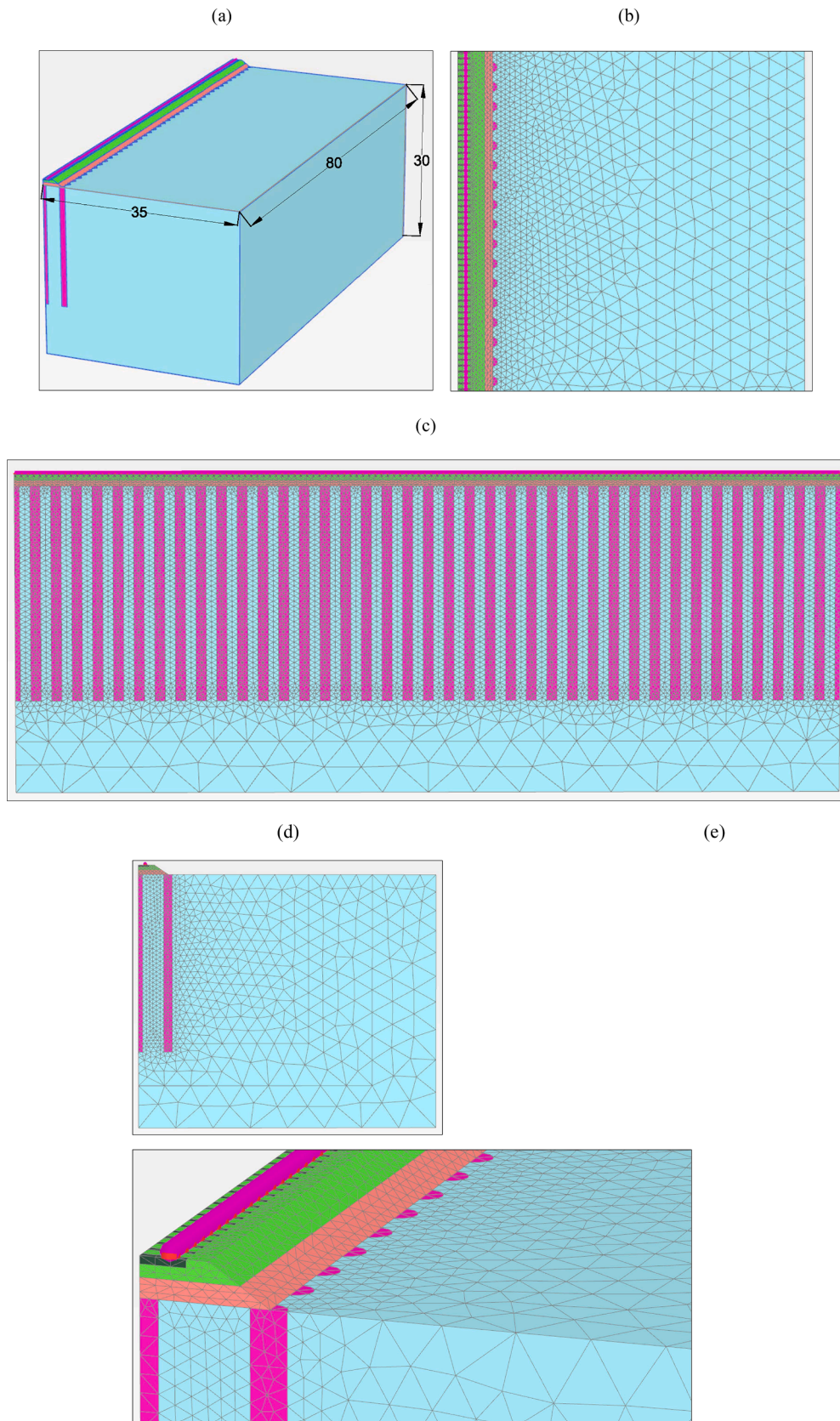


**Fig 3.** Numerical model: (a) 3D view mode (distances in metres); (b) plan; (c) longitudinal section by symmetry axis; (d) schematic cross-section; (e) detail of the ballasted track and stone column improved ground.

studying because other parameters such as rail displacement and DAF are expected to be altered. In fact, in Dong et al. [17] the effect of the stiffening of soft soils under the track has been studied for the case of a homogeneous soil, finding that the critical speed hardly varies at all with an increasing depth of the stiffening of the soil under the track, but it can be observed that the rail displacement curve tends to be asymptotic with an increasing depth of reinforcement. Also in Alves Costa et al. [5] the effect of soil improvement under the track on a homogeneous soil has been analysed, showing that the critical speed does not vary while the shakedown limit factors do decrease and to quite a high degree. In that study, the authors suggest the possibility of basing the design of the track and the limitation of the train speed on the mechanics of the track and on the shakedown theory rather than limiting it only by critical speed, since in homogeneous soils the soil improvement techniques do not lead to an appreciable increase in critical speed. In that case, the track corresponds to a slab track [5].

Regarding the geotechnical properties of non-homogeneous soil 1, a normally dispersive profile (i.e. stiffness increasing with depth) has been considered, with a linear increase in stiffness with depth and with a critical speed similar to that of the homogeneous case ( $v_{cr} = 60$  m/s). This last condition has been imposed by the authors with the aim of comparing results between a homogeneous soil and non-homogeneous soil but with the same critical speed. To estimate the increase in stiffness with depth the Ledsgard case has been considered since its critical speed is approximately 60 m/s. In this way, the non-homogeneous soil 1 corresponds to an ideal case (therefore easier to analyse) but similar to a real case with limitations in the operational speed of trains due to the geotechnical conditions. In what concerns to the stiffness value close to the ground surface (the first 2 m) has been varied by means of a parametric analysis until a critical speed and a rail displacement vs. velocity curve similar to those of the homogeneous case are obtained. In addition, the rail displacements of the static load situation for both the homogeneous soil and the non-homogeneous soil 1 have been matched.

Finally, a third soil case has been considered, corresponding to a generally dispersive profile, but with a critical speed of approximately 90 m/s (324 km/h). The choice of this scenario is justified because it corresponds to a more common case of soft soils, since cases with critical speed about 60 m/s are very scarce and should be considered as extreme cases. In this sense, a value of critical speed of 90 m/s has been considered because higher values are not especially problematic nowadays due to the current limitation in the operational speed of trains in ballasted track railways ( $\approx 80\text{--}85$  m/s). Also, after a prior parametric analysis, the values shown in Table 1 have been considered. It can be observed that, in this third case, the soil stiffness and its increase with

depth is 2.7 times greater than that of non-homogenous soil 1.

As for the stone column parameters, these have been considered in the range of very small strains and their values are in accordance with those defined in Castro [11] and in Darendeli [14].

The damping values, all of a Rayleigh type, have been considered with the usual values for these materials and are in keeping with those used in Fernández et al. (2017). Common values of the Poisson's ratio have also been assumed, namely 0.20 for the stone columns and 0.49 for the three different foundation soils as undrained conditions are assumed for these soft soils.

As for the mechanical properties of the track, these are shown in Table 2. This corresponds to a classical ballasted track, whose dynamic properties have been taken from Alves Costa et al. [3] and Fernández et al. [21].

Fig. 2 shows a schema of the Young's modulus as a function of the depth for the 3 scenarios proposed. Also, a dimensioned schema of the railway track is shown.

### Numerical model description

A 3D numerical model has been used, formulated in the time domain, using the Plaxis 3D 2018.01 software [9]. The geometry of the numerical model is shown in detail in Fig. 3 and, as can be observed, corresponds to a symmetric case, so that only half of it has been modelled. The model dimensions are 80x35x30 m in the longitudinal, horizontal and vertical directions, respectively, which are values considered and validated experimentally in 3D finite element models formulated in the time domain similar to those used here [27,19,1,42,21,23,24]. The railpad is modelled as a linear spring, with a stiffness of 600 kN/mm, while the rail has been simulated as a beam, with the standardised properties of the UIC-60 type, namely  $EA = 1.6 \cdot 10^6$  kN and  $EI = 6.4 \cdot 10^3$  kN\*m<sup>2</sup>. The rest of the track components (sleeper, ballast and subballast) and the ground and stone columns were modelled using 3D solid elements. The axis-to-axis spacing between sleepers in the longitudinal direction is 0.6 m and their width is 0.2 m. All of the materials are modelled assuming a linear elastic behaviour, as has been considered in most research on critical speed ([4,5,17,6,40]; among others). In this regard, it should be noted that there are very few studies on the effect of the non-linear soil behaviour on the critical speed [18,2,42] showing a moderate influence (about 10–15%) but with a very high computational cost. In addition, in the case of soil reinforcement the shear strains induced in the ground are small, therefore causing a negligible influence the non-linear soil behaviour.

As is well known, in any dynamic analysis the element size, the boundary conditions and the dynamic time step have to be chosen carefully to guarantee an acceptable accuracy in the results (e.g., [25]). The finite element mesh used in this paper is unstructured (Fig. 3). Tetrahedral 10-node elements are used and a minimum element size in the ground of 0.4 m (in the area around the track) has been considered to allow a simulation of high frequency movements. In general, the frequencies at which the critical speed phenomenon occurs in soft soils are low, between 0 and 20 Hz. In this way, the model is made up of 437,071 elements and 621,670 nodes. The boundary conditions correspond to viscous dampers [37,34] in all boundaries except in the plane of symmetry, where horizontal movements are impeded, and the ground surface, which is a free boundary. The damping of the ground has been considered according to a Rayleigh type, very suitable and widely used in numerical models formulated in the time domain (e.g., [1]).

As regards the numerical modelling of the moving loads, this has been applied according to the equivalent nodal force method, in keeping with that described in Galavi and Bringreva (2014) and the time step has been considered according to the criteria of Courant-Friedrichs-Lewy [25,1] with an implicit Newmark integration scheme, shown below:

$$C_n = \frac{\Delta t v_x}{L_{min}} < 1 \tag{1}$$

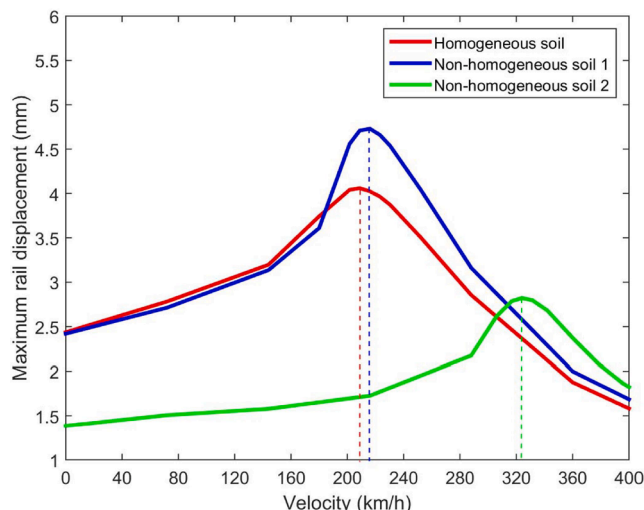


Fig. 4. Maximum rail displacement vs. train velocity for 3 soils.

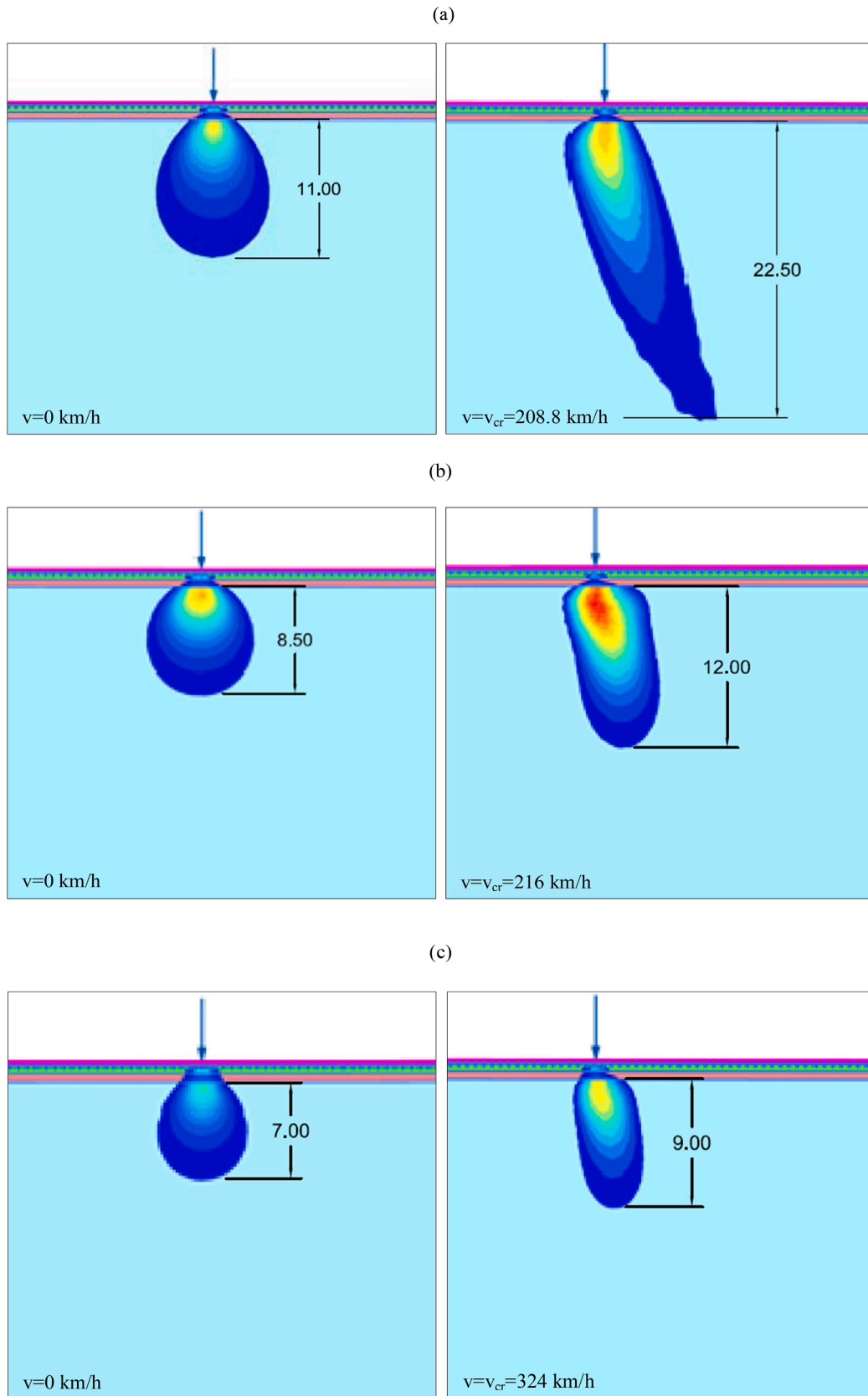


Fig. 5. Depth of pressure bulb: (a) homogeneous soil; (b) non-homogeneous soil 1; (c) non-homogeneous soil 2 (left: static case; right: dynamic case corresponding to critical speed) (in meters).

**Table 3**  
Depth of pressure bulb for 3 soils.

	Homogeneous soil	Non-homogeneous soil 1	Non-homogeneous soil 2
Depth of “static” pressure bulb ( $L_{sb}$ )	11.00 m (4.4B)	8.50 m (3.4B)	7.00 m (2.8B)
Depth of “dynamic” pressure bulb ( $L_{db}$ )	22.50 m (9.0B)	12.00 m (4.8B)	9.00 m (3.6B)
$L_{db}/L_{sb}$	2.0	1.4	1.3
Resonant frequency (Hz)	5.55	6.93	9.98

where:  $C_n$  is the Courant number,  $\Delta t$  is the dynamic time step,  $v$  is the speed of the moving load and  $L_{min}$  is the distance between two adjacent loading nodes.

It should be noted that in all cases the train is modelled as a moving 200 kN axle load, so that all results are for a single wheel passage only. This is acceptable for linear simulations [18] such as those performed in this study. The load induced by trains is made up of the quasi-static and dynamic load (caused by rail irregularities, wheel flats, welds, etc.). As shown by Lombaert and Degrande [36], Kece et al. [32] and Alves Costa et al. [5] the quasi-static excitation is the dominant factor in the response of the track, compared to the dynamic excitation, which contributes mainly to the free-field response. Therefore, for the analysis of critical speed and rail displacements it is acceptable to neglect the dynamic excitation according to the usual hypotheses used in most studies on critical speed in railway lines [27,2,4,1,42] among others).

**Results without stone columns**

The results obtained for rail displacement vs. velocity for the three cases studied are shown in Fig. 4.

As can be seen in Fig. 4, the critical speed for the homogeneous soil is 208.8 km/h (58 m/s), for non-homogeneous soil 1 it is 216 km/h (60 m/s) and for non-homogeneous soil 2 it is 324 km/h (90 m/s). In the following, the train velocities will be given in km/h as is common practice. The frequencies at which the critical speed phenomenon occurs are 5.55, 6.93 and 9.98 Hz, respectively. Logically, the rail displacements are smaller on the stiffer ground and the critical speed is higher the greater the stiffness of the underlying soil. Comparing the homogeneous and the non-homogeneous soil 1, it can be seen that their rail displacement vs. velocity curves are practically identical up to a velocity of 180 km/h, increasing more sharply for the case of non-homogeneous soil 1 until reaching the critical speed, due mainly to the lower stiffness of the soil in the first 2 m of depth. However, the differences of the rail displacement vs velocity curves between the non-homogeneous soil 1 and the non-homogeneous soil 2 are considerable because the maximum rail displacement for non-homogeneous soil 2 is practically half of that for non-homogeneous soil 1. Furthermore, the peak of the rail displacement of the non-homogeneous soil 2 is located for a higher velocity than in the case of non-homogeneous soil 1. The reason for these differences lies in a greater stiffness of non-homogeneous soil 2 than non-homogeneous soil 1. Regarding the shape of the curves, these are similar although the non-homogeneous soil 1 shows a slightly sharper shape than the non-homogeneous soil 2.

Fig. 5 shows the pressure bulbs obtained for the 3 soils, both for the static case ( $v = 0$  km/h) and for the dynamic case corresponding to the critical speed. It should be noted that the pressure bulb has been considered here as the locus of the points whose stress increase is 10% of the maximum stress increase experienced in the soil, except for the materials that make up the railway track (ballast and sub-ballast). Table 3 summarises the maximum depth of the pressure bulb for each studied case. The pressure bulb is a term applied in foundation

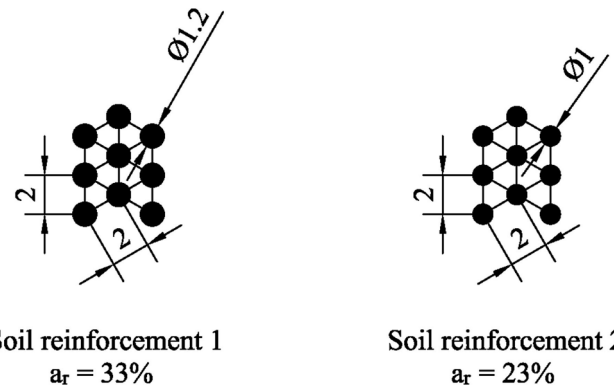


**Fig. 6.** Scheme of the two types of stone column configurations (distances in meters).

engineering for static loads and for elastic-linear behaviour. However, here it is also considered for dynamic cases, so that it could be named as a “dynamic” pressure bulb. The objective of comparing the critical speed cases with the static cases is simply due to the fact that the classical pressure bulb concept is for static cases, it being evident that for the case of railway vibrations the static case is less deep.

As can be seen (Table 3), the depth of the “static” pressure bulb ( $L_{sb}$ ) varies between 2.8 and 4.4B, where B is the width of the loaded zone, which in this case has been taken to be equal to the length of the sleeper, whose value is equal to 2.5 m. Expressing the pressure bulb and the critical length as a function of the loaded area is a common practice [12] and has therefore also been used in this study. On the other hand, for moving loads and specifically for critical speed, the depth of the dynamic pressure bulb ( $L_{db}$ ) ranges from 3.6B to 9B. In this sense, the dynamic scenario and specifically for critical speed situation leads to an elongation of the pressure bulb with respect to the static one, which in terms of dynamic amplification ( $L_{db}/L_{sb}$ ) implies a factor of 2 for the homogeneous soil and of 1.3–1.4 for the non-homogeneous soils. The elongation of the dynamic pressure bulb takes place both in the vertical direction and in the direction of movement of the load. These dynamic amplification factors for the depth of the pressure bulb are smaller the stiffer the soil is, since the frequency at which the critical speed phenomenon occurs is higher, leading to a shorter wavelength and, therefore, a smaller dynamic pressure bulb. In this sense, there is a clear relation between resonant frequency and pressure bulb depth (Table 3).

**Effects of stone columns**

To study the effects of stone columns, two typical configurations for soil reinforcement have been considered for each of the three proposed soil profiles (Fig. 2a). The same triangular grid has been considered for both cases, only varying the diameter of the stone columns. These cases can be seen in Fig. 6 and are defined by their area replacement ratio ( $a_r$ ). To perform the parametric analyses and to study the column critical length, the length of the columns has been varied in increments of 1.5 m, starting at 0 m and going up to 21 m. The maximum column length was chosen based on two criteria: i) range of column lengths used in practice (e.g. [8] and ii) because a length greater than 21 m does not cause any improvement in terms of critical speed or rail displacements for the cases studied in this paper.

The effects of the stone columns have been studied using three parameters: rail displacement, DAF and critical speed. The results obtained in each of the three soil cases studied are analysed below.

*Homogenous soil*

Fig. 7 shows the rail displacement vs. velocity for the homogeneous soil for both  $a_r$  values. Since it corresponds to an inversely dispersive

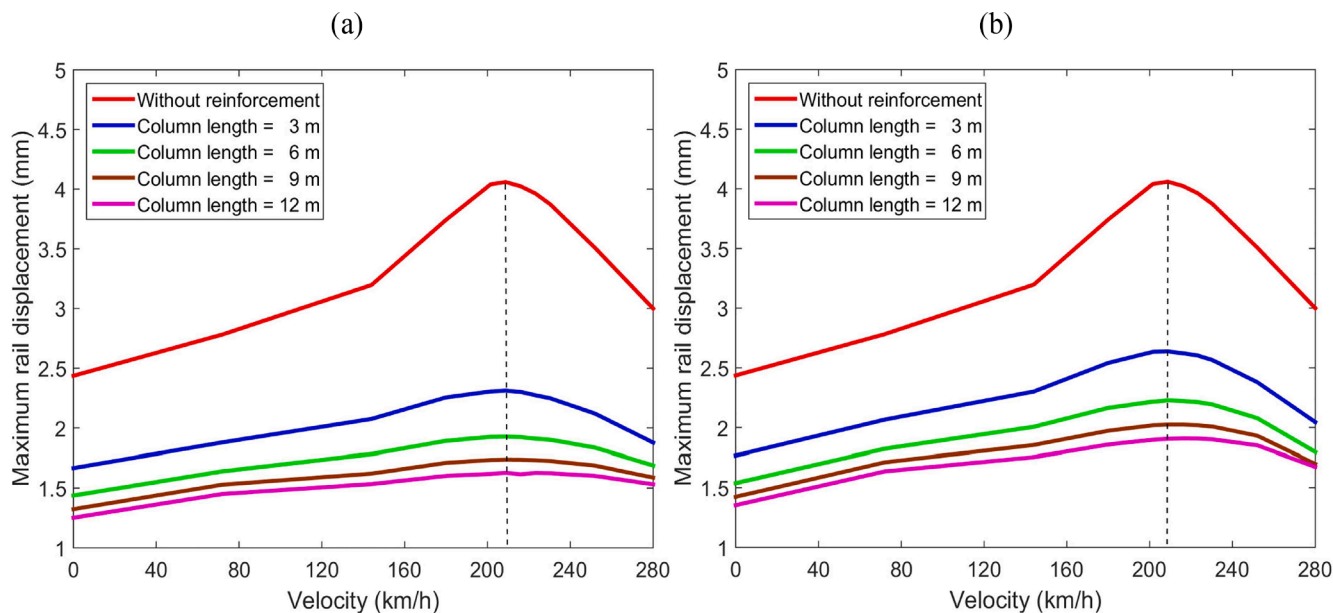


Fig. 7. Maximum rail displacement vs. velocity for homogeneous soil: (a)  $a_r = 33\%$ ; (b)  $a_r = 23\%$

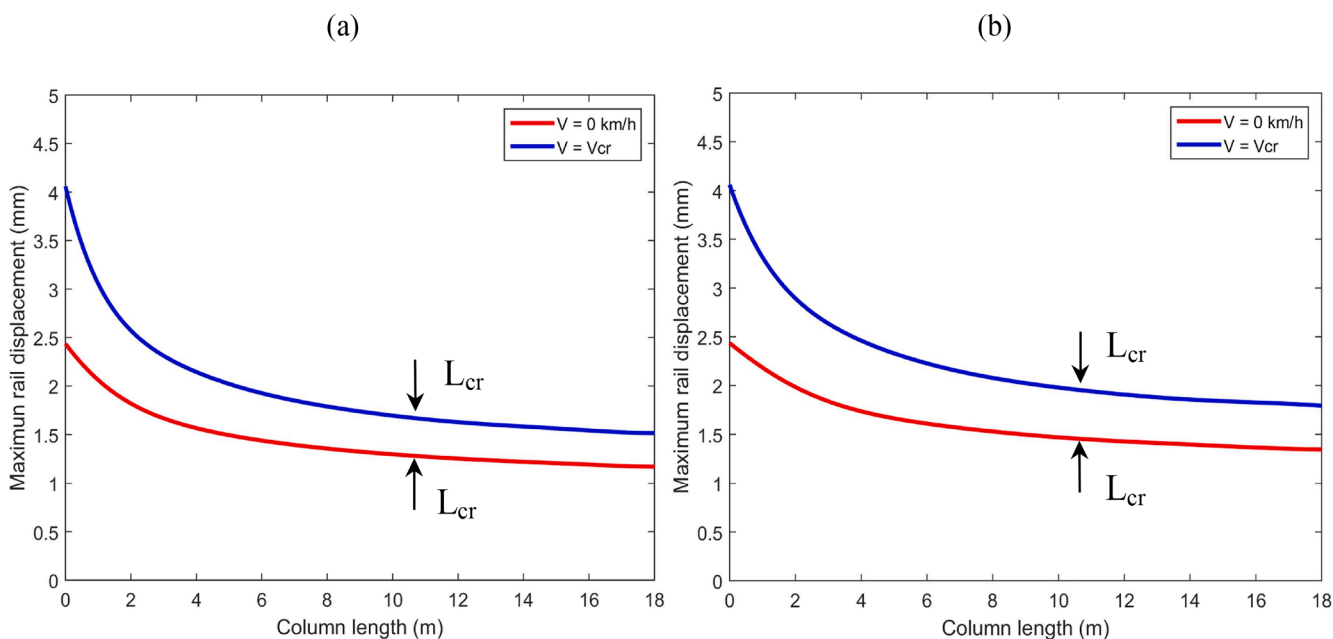


Fig. 8. Maximum rail displacement vs. column length for homogeneous soil: (a)  $a_r = 33\%$ ; (b)  $a_r = 23\%$

case, the critical speed remains constant when the ground is reinforced with stone columns as the layer below the reinforcement zone is the one that determines the critical speed and, in this case, this is 208.8 km/h. Fig. 7 only shows the curves up to a length of stone column of 12 m because curves corresponding to greater lengths of stone columns would be very close to each other.

Comparing the results for both  $a_r$  (Fig. 7), it is observed that a higher  $a_r$  produces a greater decrease in the rail displacement, as expected. However, it can be appreciated how the distance between the different curves for different column lengths ( $L$ ) represented in Fig. 7 decreases as  $L$  increases. This fact indicates that, based on the maximum rail displacement, there could be a critical length. This can be seen in more detail in Fig. 8 where the maximum rail displacement vs. column length is shown, both for the static case and for the dynamic case corresponding to the critical speed and for both  $a_r$ . The results of the static case have

been shown for comparison. In these cases, where the curve becomes asymptotic with increasing length, but without becoming fully horizontal, the criterion for its determination has been to consider as the critical column length ( $L_{cr}$ ) the value for which the rail displacement is 10% greater than the minimum found. It can be seen how  $L_{cr}$  for the dynamic case is approximately 10.5 m for both area replacement ratios. Comparing this value with that which corresponds to the static case, it can be seen how the “dynamic” critical length is similar to the static one. Furthermore, it can be seen how  $a_r$  has a negligible influence on  $L_{cr}$  for the studied cases.

As regards the DAF, which is the relation between the rail displacement for the critical speed and the rail displacement for the static load, Fig. 9 shows its value for both area replacement ratios as a function of the column length, always for the case of the critical speed ( $v = v_{cr}$ ). It can be observed how  $L_{cr}$  with respect to the DAF is around 12 m



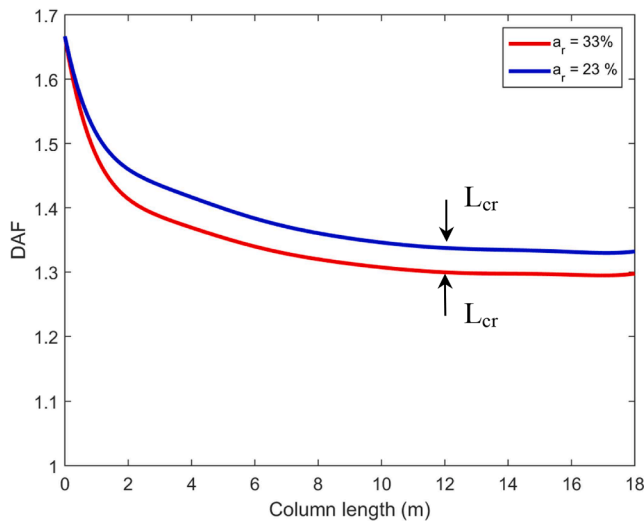


Fig. 9. DAF vs. column length for homogeneous soil.

Table 4  
Critical length of stone columns for homogeneous soil.

	$a_r = 33\%$	$a_r = 23\%$
$L_{cr}$ according to rail displacement	10.5 m	10.5 m
$L_{cr}$ according to DAF	12.0 m	12.0 m
$L_{cr}$ according to $v_{cr}$	—	—

for both  $a_r$  values, since the wavelength of the Rayleigh waves associated to the resonant frequency is approximately of this length. As expected, a greater  $a_r$  implies a slightly lower DAF. In contrast,  $L_{cr}$  does not seem to appreciably depend on  $a_r$  for the cases analysed.

In view of the results for the homogeneous case, it may be stated that there is not one single concept of critical length of stone columns in the case of high-speed railway lines since this length may be different as a function of the parameters with which it is evaluated and the specific criterion used for its determination. In this case, it would seem reasonable to propose a requirement to implement 3 different critical lengths: i) according to rail displacement; ii) according to DAF and iii) according

to critical speed. In the particular case of the homogeneous soil studied here, there is no critical length with respect to the critical speed as this is constant since it corresponds to an inversely dispersive case.

The three different critical lengths found for the case of the homogeneous soil are gathered in Table 4.

Non-homogeneous soil 1

Fig. 10 shows rail displacement vs. train (load) velocity for the non-homogeneous soil 1 for both replacement rates. Since in this case it corresponds to a normally dispersive case, the critical speed increases when the soil is reinforced with stone columns. In fact, a change in the critical speed is observed from 216 km/h (case without columns) to 295 km/h ( $L = 18$  m and  $a_r = 23\%$ ) and up to 327.6 km/h ( $L = 18$  m and  $a_r = 33\%$ ). Here, the effect of the stone columns is clear and sharp, increasing the critical speed value by up to 52%. It can also be observed how a higher  $a_r$  implies a greater increase in the critical speed, since the stiffness of the improved soil is greater.

As in the case of the homogeneous soil, it can be observed how the distance between the different curves represented (Fig. 10) decreases as the length of the stone columns increases. This fact would again seem to indicate that, based on the maximum rail displacement, there is also a critical length of the stone columns. This can be seen in more detail in Fig. 11 where the maximum rail displacement vs. column length is shown, both for the static case and for the dynamic case corresponding to the critical speed and for both  $a_r$  values. It can be seen how the critical length for the dynamic case is approximately 10 m for both  $a_r$ . In the same way as in the case of homogeneous soil, it can be observed that  $a_r$  has a negligible influence on  $L_{cr}$ .

As for the DAF, Fig. 12 shows its value for both  $a_r$ , in all cases for the critical speed. It can be observed how  $L_{cr}$  with respect to the DAF is around 9 m for both  $a_r$ , as the energy of the Rayleigh waves has almost completely dissipated at this depth. A greater length of column implies a lower DAF and, for a higher  $a_r$ , it is observed that the DAF is slightly lower. In contrast,  $L_{cr}$  does not nearly depend on  $a_r$ .

As mentioned previously, in this case of a non-homogeneous soil, an increase in the length of the stone columns implies an increase in the critical speed. To quantify this fact more accurately, these values have been gathered in Fig. 13, where the critical speed is shown as a function of the length of the stone columns for both replacement rates. It can be seen that the effect of the stone columns on the critical speed is clear, the

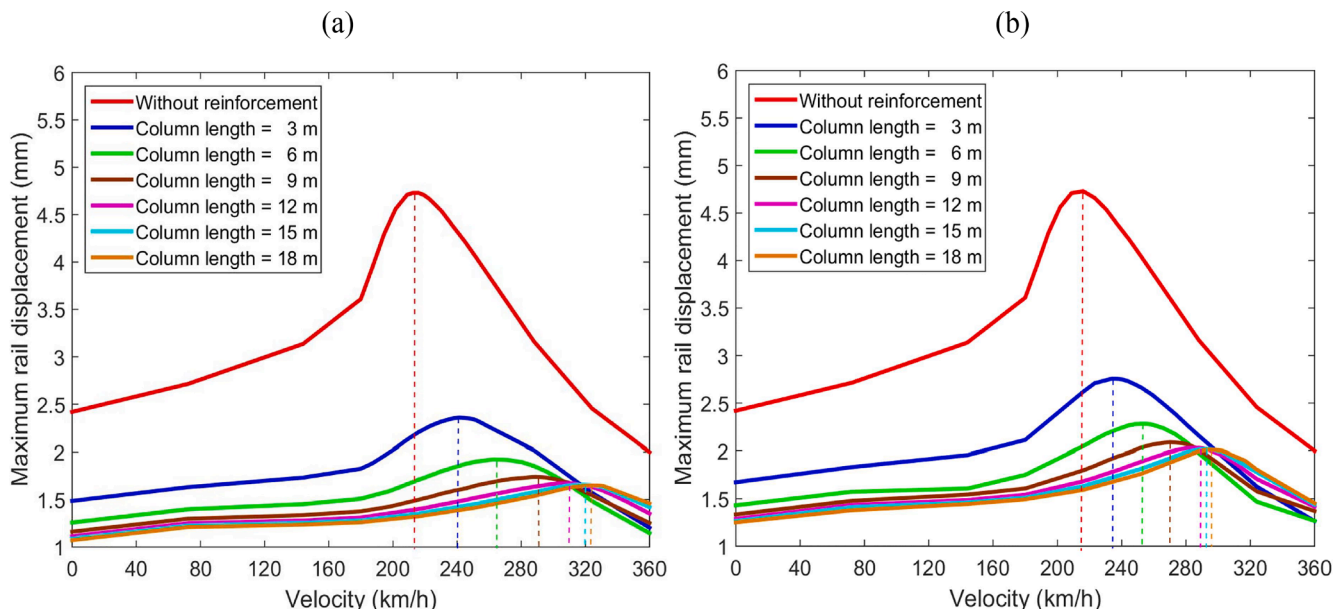


Fig. 10. Maximum rail displacement vs. velocity for non-homogeneous soil 1: (a)  $a_r = 33\%$ ; (b)  $a_r = 23\%$

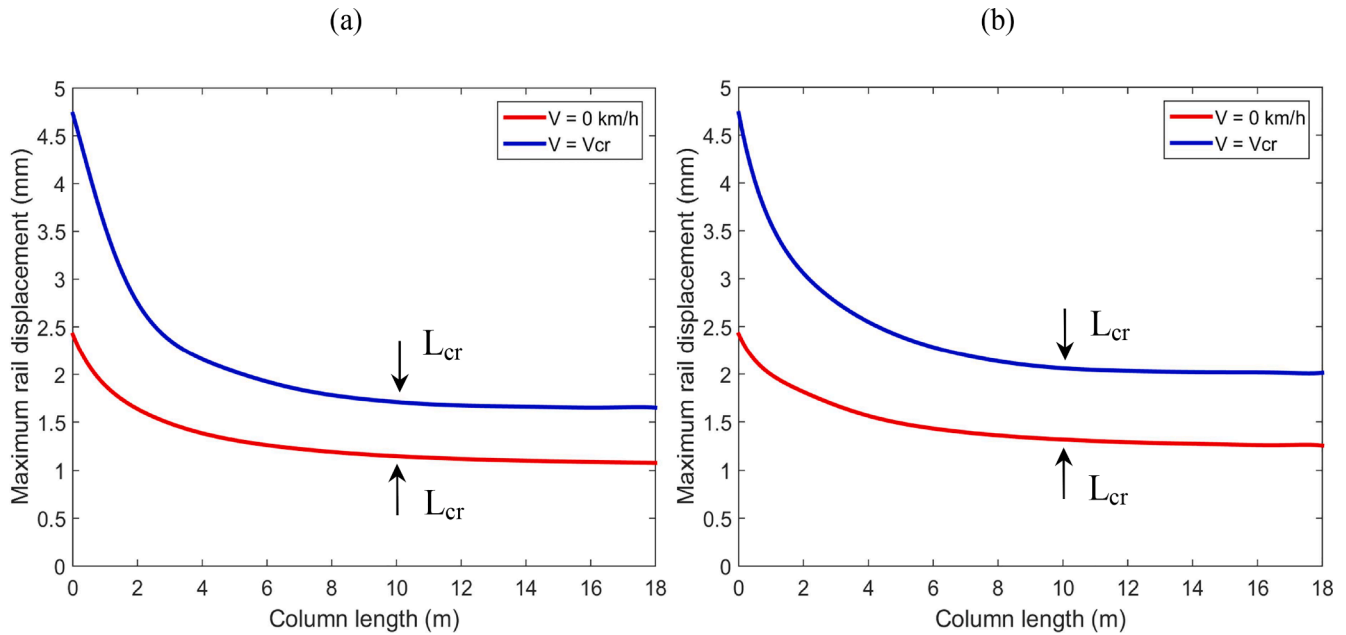


Fig. 11. Maximum rail displacement vs. column length for non-homogeneous soil 1: (a)  $a_r = 33\%$ ; (b)  $a_r = 23\%$

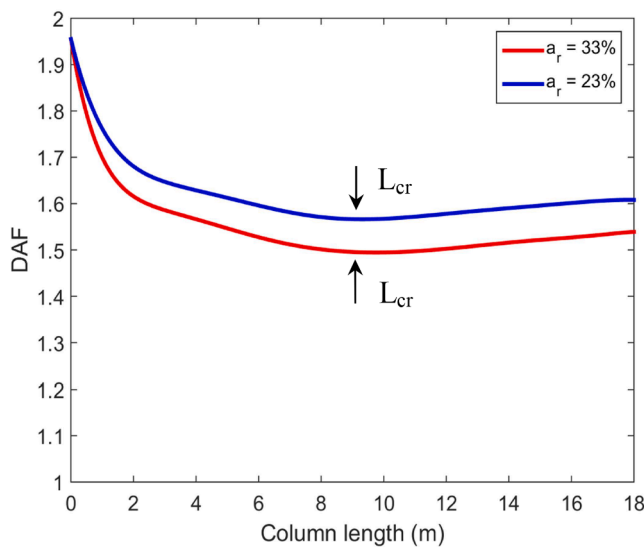


Fig. 12. DAF vs. column length for non-homogeneous soil 1.

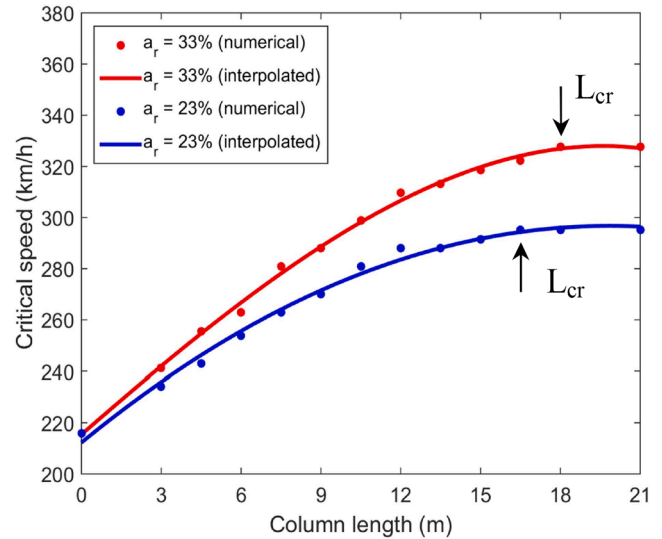


Fig. 13. Critical speed vs. column length for non-homogeneous soil 1.

latter increasing with increasing length. This increase is not indefinite and has a limit, corresponding to 16.5 m and 18 m for  $a_r = 23\%$  and  $33\%$ , respectively. The increase is approximately linear up to a depth of 12 m, from which the curve becomes asymptotic until reaching the value of the critical length. In this sense, deepening the reinforcement more than 12 m is less efficient as the energy of the Rayleigh wave is confined close to the soil surface. Quantitatively, the critical speed goes from 216 km/h to 295 km/h (for  $a_r = 23\%$ ) and to 327.6 km/h (for  $a_r = 33\%$ ). In this sense, a higher replacement rate causes a greater increase in critical speed, since the reinforced ground is stiffer. In percentage terms, the critical speed increases by 37% for  $a_r = 23\%$  and by 52% for  $a_r = 33\%$ .  $L_{cr}$  is slightly higher for a higher  $a_r$ .

In this case of a non-homogenous soil, it is even more clear that the concept of critical length in high-speed railway lines must be established in reference to the three parameters analysed: maximum rail displacement, DAF and critical speed. Table 5 gathers the values found for critical column length for this case, commented on previously, in which

Table 5

Critical length of stone columns for non-homogeneous soil 1.

	$a_r = 33\%$	$a_r = 23\%$
$L_{cr}$ according to rail displacement	10.0 m	10.0 m
$L_{cr}$ according to DAF	9.0 m	9.0 m
$L_{cr}$ according to $v_{cr}$	18.0 m	16.5 m

it can be observed how the threshold value is for  $v_{cr}$  since it leads to a higher critical length. However, after 12 m of length, the effectiveness of the columns in terms of the increase in critical speed is moderate.

An interesting analysis can be made by looking at Fig. 14, which shows the pressure bulbs obtained for three different stone column lengths: 15, 18 and 21 m, for the replacement rate  $a_r = 33\%$  and for their critical speed. It can be seen that below the critical length (with respect to the critical speed) the pressure bulb reaches a depth greater than the length of the column. However, for a column length greater than the

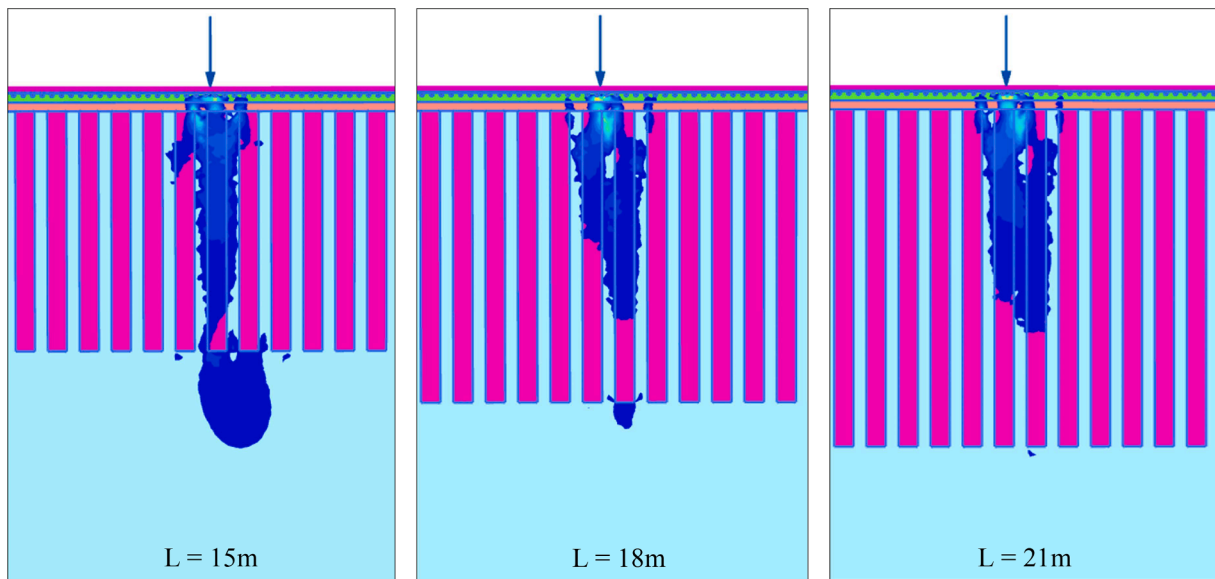


Fig. 14. Depth of pressure bulb for  $v_{cr}$  for non-homogeneous soil 1 with  $a_r = 33\%$

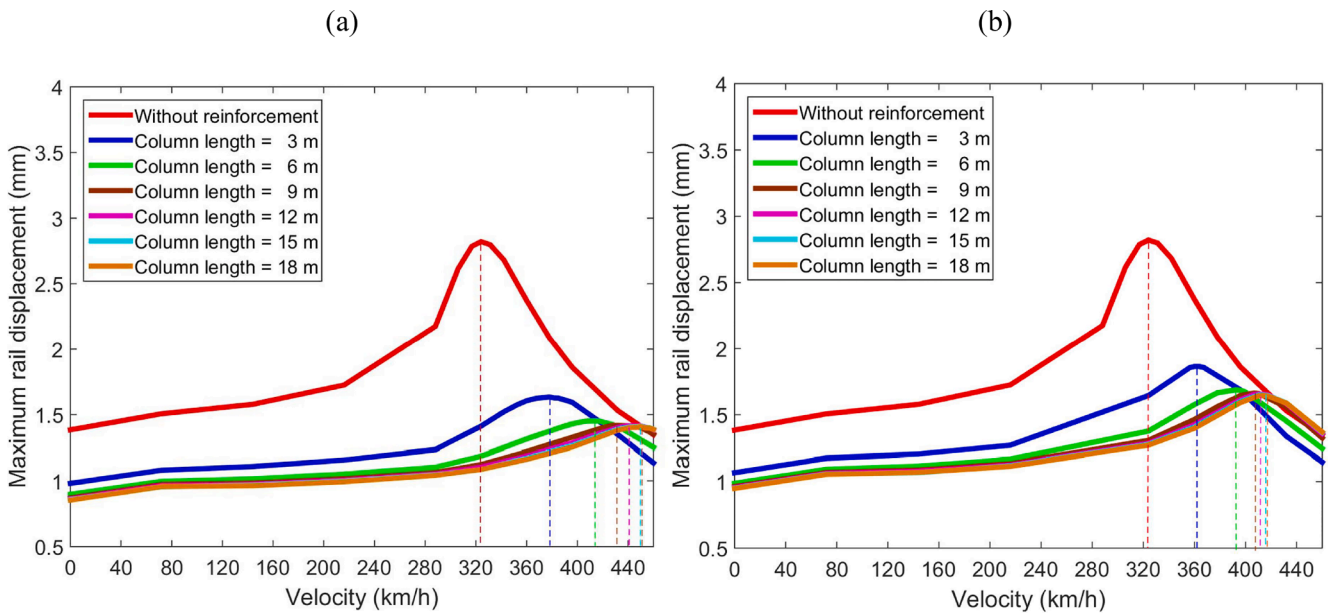


Fig. 15. Maximum rail displacement vs. velocity for non-homogeneous soil 2: (a)  $a_r = 33\%$ ; (b)  $a_r = 23\%$

critical length, the pressure bulb no longer reaches the length of the columns. In the case of the critical length, the pressure bulb practically coincides with the length of the columns. The pressure bulb for the non-homogeneous soil 1 without reinforcement reaches 12 m (Fig. 5b). As can be seen, the pressure bulb “deepens” when the soil is reinforced with stone columns, transmitting the load to the lower part of these. This fact is relevant because it implies that the critical column length is larger than the depth of the pressure bulb for the non-improved case. This same analysis can be performed for  $a_r = 23\%$ , with very similar results to the one discussed here. For this reason, it is not included here and can be consulted in the [supplementary material \(S1\)](#).

*Non-homogeneous soil 2*

Regarding the results obtained for the stiffer non-homogenous soil, Fig. 15 shows the rail displacement vs. velocity for both are replacement ratios. In this case, the critical speed ranges from 324 km/h (case

without columns) up to 414 km/h (for  $a_r = 23\%$ ) y 450 km/h (for  $a_r = 33\%$ ). The effect of the stone columns is significant since it leads to increases of around 39% in the critical speed value, although as shall be seen below, this is proportionally lower than for the above case (non-homogeneous soil 1), as the difference between the stiffness of the columns and the soil is smaller. A higher replacement rate leads to a greater increase in the critical speed, as the average stiffness of the improved soil is greater and, logically, corresponds to a normally dispersive ground scenario.

As in the other two soil stiffness profiles, it can be observed how the distance between the different curves represented in Fig. 15 decreases as the length of the stone columns increases. Fig. 16 shows the maximum rail displacement vs. column length, for both the static case and the dynamic case corresponding to the critical speed and for both  $a_r$ . It can be observed how the critical length for the dynamic case is approximately 7 m for both  $a_r$ . As in the two previous cases,  $a_r$  does not appreciably influence the critical length  $L_{cr}$  for the studied cases.

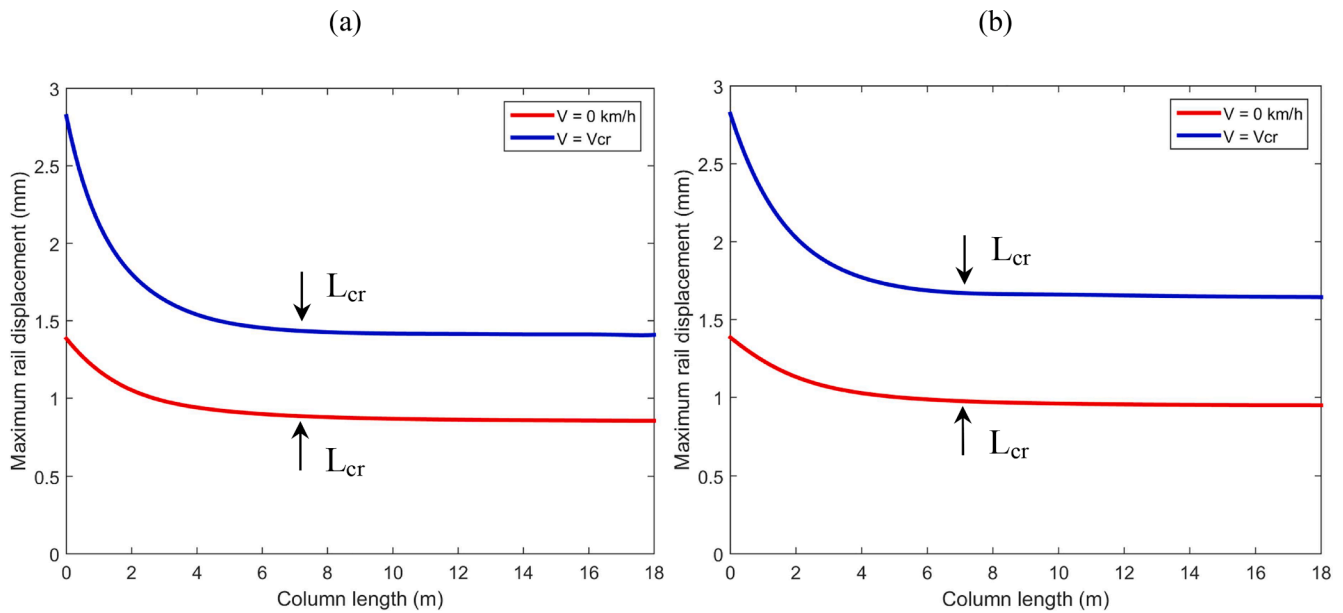


Fig. 16. Maximum rail displacement vs. column length for non-homogeneous soil 2: (a)  $a_r = 33\%$ ; (b)  $a_r = 23\%$

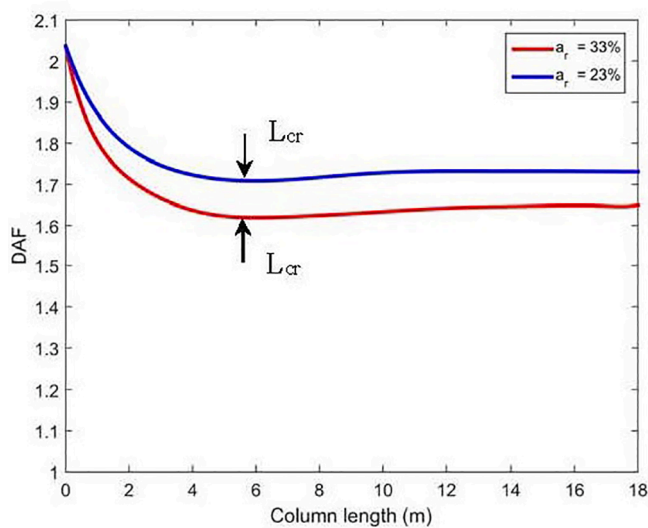


Fig. 17. DAF vs. column length for non-homogeneous soil 2.

Fig. 17 shows the DAF vs. column length for both  $a_r$ . A critical column length with respect to the DAF of 5.5 m can be observed for both  $a_r$ . It can also be seen that for a higher  $a_r$ , the DAF is again slightly smaller. In contrast, the critical length does not depend on  $a_r$ , as occurred in the two previous cases.

Fig. 18 shows the critical speed as a function of the length of the stone columns for both replacement rates. The effect of these on the critical speed is significant, this speed increasing with an increase in length. This increase is not indefinite and has a limit, corresponding to 13.5 m for both  $a_r$ . Quantitatively, the critical speed goes from 324 km/h at 414 km/h (for  $a_r = 23\%$ ) and to 450 km/h (for  $a_r = 33\%$ ). Thus, a higher replacement rate leads to a greater increase in the critical speed, in a similar way to that of the case of non-homogeneous soil 1. The increase is approximately linear up to a depth of 6 m, due to the fact that the Rayleigh wave energy is confined close to the surface, and after this value the curve becomes asymptotic until it reaches the value of the critical length. In percentage terms, the critical speed increases by 28% (for  $a_r = 23\%$ ) and by 39% (for  $a_r = 33\%$ ). However, the critical length

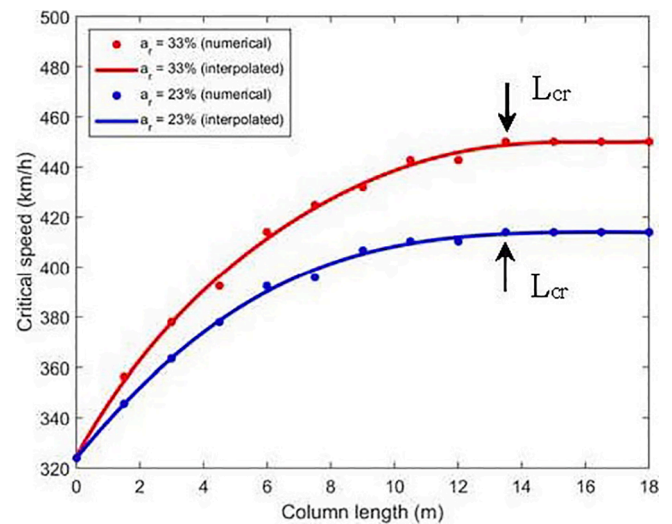


Fig. 18. Critical speed vs. column length for non-homogeneous soil 2.

Table 6  
Critical length of stone columns for non-homogeneous soil 2.

	$a_r = 33\%$	$a_r = 23\%$
$L_{cr}$ according to rail displacement	7.0 m	7.0 m
$L_{cr}$ according to DAF	5.5 m	5.5 m
$L_{cr}$ according to $v_{cr}$	13.5 m	13.5 m

does not seem to depend significantly on  $a_r$ .

Table 6 gathers the values obtained for the critical length according to the three parameters analysed. As in the case of non-homogeneous soil 1, the least favourable critical length is with respect to the critical speed.

Fig. 19 shows the pressure bulbs obtained for 3 different stone column lengths: 9, 13.5 and 18 m, for the replacement rate  $a_r = 33\%$  and for the critical speed. As in the case of non-homogeneous soil 1, the results show how, for stone column lengths lower than the critical length for the critical speed, the pressure bulb comfortably surpasses the column length, while for the opposite situation the pressure bulb does not reach the total length of the columns. These results coincide fully with those

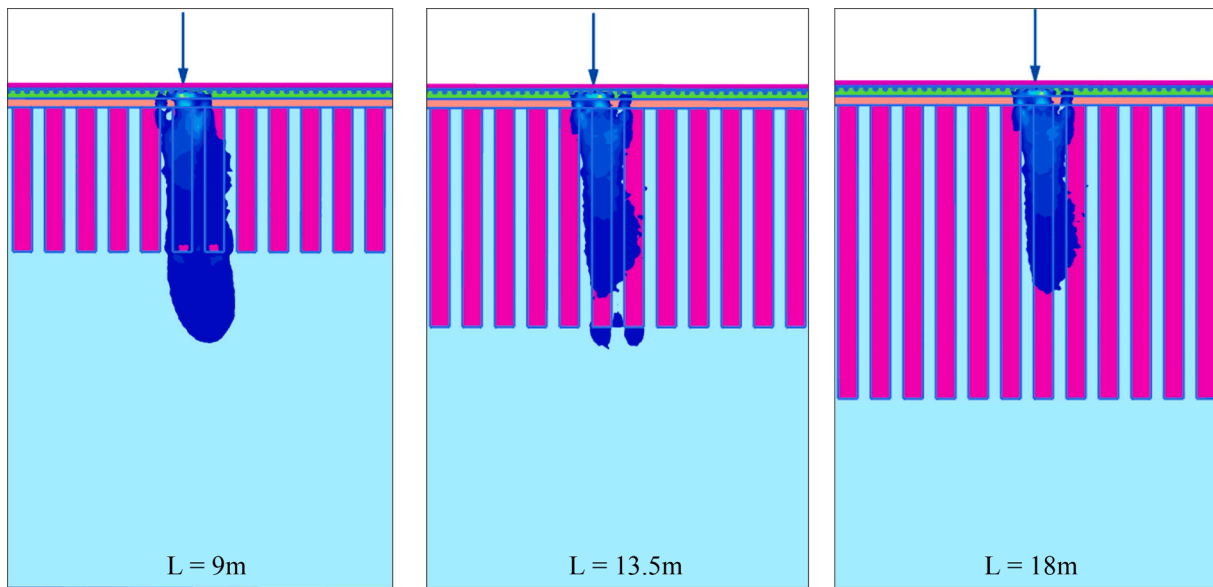


Fig. 19. Depth of pressure bulb for  $v_{cr}$  for non-homogeneous soil 2 with  $a_r = 33\%$

Table 7  
Critical length of stone columns for 3 soils.

	Homogeneous soil		Non-homogeneous soil 1		Non-homogeneous soil 2	
	$a_r = 33\%$	$a_r = 23\%$	$a_r = 33\%$	$a_r = 23\%$	$a_r = 33\%$	$a_r = 23\%$
$L_{cr}$ for rail displacement	10.5 m	10.5 m	10.0 m	10.0 m	7.0 m	7.0 m
$L_{cr}$ for DAF	12.0 m	12.0 m	9.0 m	9.0 m	5.5 m	5.5 m
$L_{cr}$ for $v_{cr}$	—	—	18.0 m	16.5 m	13.5 m	13.5 m
Depth of dynamic pressure bulb without reinforcement ( $L_{db}$ )	22.50 m		12.00 m		9.00 m	

Table 8  
Resonant frequencies.

Homogeneous soil		Non-homogeneous soil 1		Non-homogeneous soil 2	
Without stone columns	With stone columns	Without stone columns	With stone columns	Without stone columns	With stone columns
5.55 Hz	9.98 Hz	6.93 Hz	9.98 Hz	9.98 Hz	20.53 Hz

obtained for the non-homogenous soil 1 and confirm the analysis made. As for the results obtained for  $a_r = 23\%$ , these are practically identical to those shown and hence they are omitted here and can be consulted in the supplementary material (S2).

Discussion

Throughout this study, the critical length of stone columns has been analysed for the three different soils according to three different parameters: i) maximum rail displacement; ii) DAF and iii) critical speed. Table 7 gathers the critical lengths obtained and also shows the depth of the dynamic pressure bulb for the three cases without reinforcement.

It can be observed how the natural soft soil stiffness leads to a

reduction in the critical lengths for the three parameters studied. The reason for this lies in the fact that for a greater soil stiffness the critical speed phenomenon occurs at a higher frequency, corresponding to a shorter wavelength and thus to a lower affected ground length, since the energy of the Rayleigh waves is dissipated at a lower depth. This increase in frequency can be observed in Table 8, which shows the resonant frequencies for each of the soils, both for the case without reinforcement and for the reinforced case for the critical length and for  $a_r = 33\%$ .

Also, this fact can be explained by the contrast in stiffness between the stone column and the soil. A greater contrast in stiffness implies a higher stress concentration ratio, which is defined as (e.g., [28]):

$$n = \frac{\Delta\sigma_c}{\Delta\sigma_s} \tag{2}$$

where  $\Delta\sigma_c$  and  $\Delta\sigma_s$  are the increase in vertical stress in the column and in the soil, respectively.

Fig. 20 shows the vertical stress values on the ground surface (plan view) for the non-homogenous soil 1 ( $L = 18$  m and  $v = v_{cr} = 327.6$  km/h) and for the non-homogenous soil 2 ( $L = 13.5$  m and  $v = v_{cr} = 450$  km/h). It can be observed that there is a higher concentration of vertical stress in the stone columns and a lower stress in the case of the softest soil (non-homogeneous soil 1), thus leading to a higher stress concentration ratio and a greater critical length.

Once the results in the 3 scenarios have been globally analysed, it is worth comparing the critical length values between the two non-homogeneous soils. As can be seen in Table 7, the critical length of non-homogeneous soil 2 is smaller than that for the non-homogeneous soil 1 for all the studied parameters. Moreover, the differences found in the critical length for both scenarios are relevant, being of 40% for rail displacement, 30% for DAF and 20–28% for critical speed. In addition, the most restrictive value of the critical length is the related to the critical speed. The relationship between critical length for critical speed and for DAF and rail displacement is similar on both soils. In this sense, the soil stiffness plays a very important role in the critical length of stone columns under ballasted track railways, implying that as the soil stiffness increases the critical length decreases. The  $a_r$  has a minor influence on the critical length.

An exception can be found in the critical length for the case of the homogenous soil, where the inversely dispersive profile of the reinforced soil implies that the critical speed remains constant.

Relating the critical length with the dynamic pressure bulb of the soil

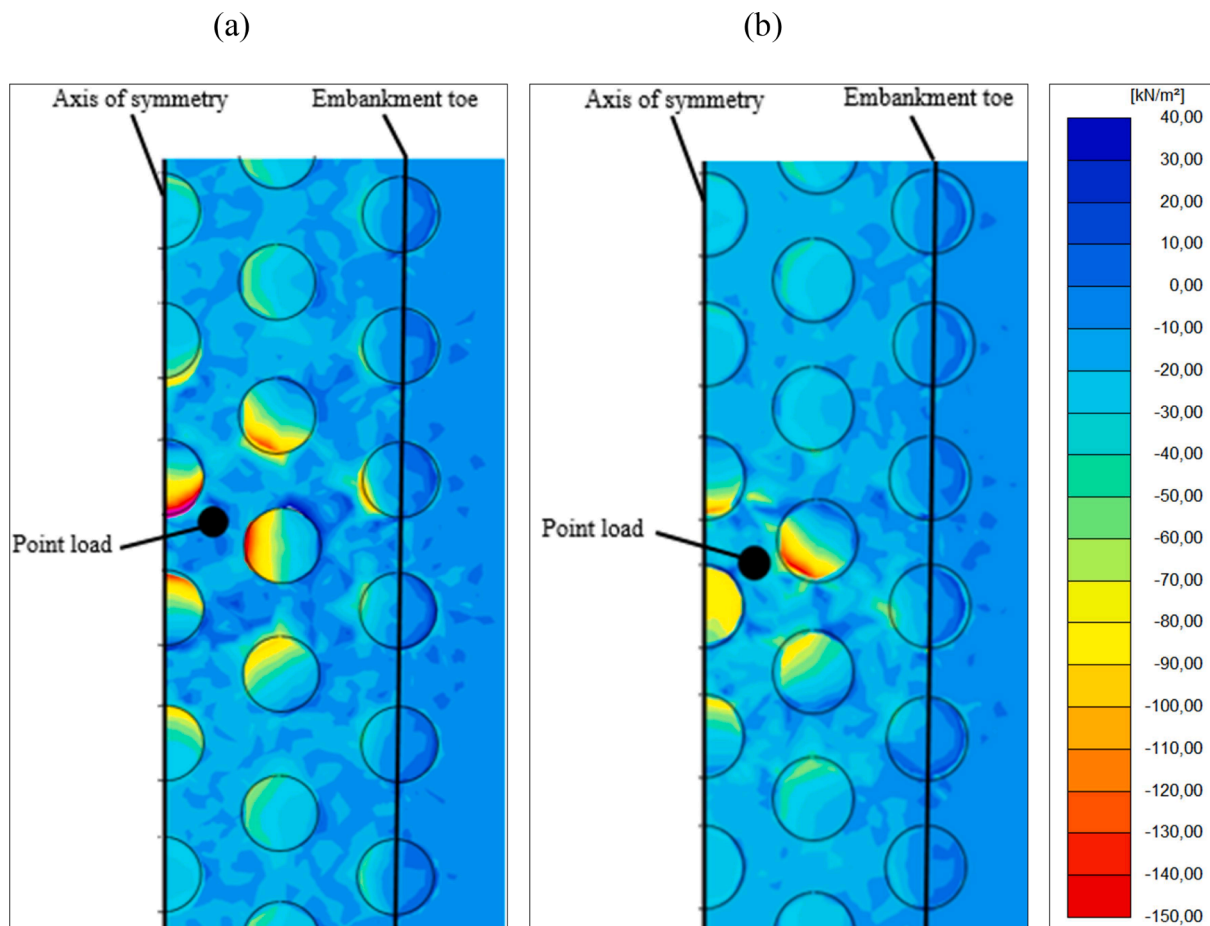


Fig. 20. Contours of the vertical stress on ground surface (plan view): a) Non-homogeneous soil 1 ( $L = 18$  m and  $v = v_{cr} = 327.6$  km/h); b) Non-homogeneous soil 2 ( $L = 13.5$  m and  $v = v_{cr} = 450$  km/h).

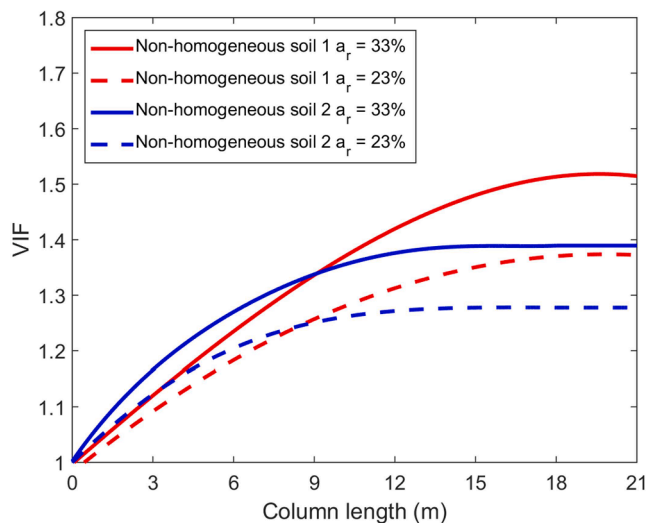


Fig. 21. Comparison of critical speed improvement factor for the non-homogeneous soils.

without reinforcement, it can be observed how for the non-homogeneous cases, the  $L_{cr}/L_{db}$  ratio for the critical speed ranges from 1.5 to 1.4 for the non-homogeneous soil 1 and is 1.5 for the non-homogeneous soil 2. Logically, this relation is not possible in the homogenous case as there is no critical length with respect to the critical speed.

Here, a critical speed improvement factor (VIF) is introduced to

evaluate the increase in the critical speed achieved with the stone column treatment:

$$VIF = \frac{v_{cr, reinf}}{v_{cr, no reinf}} \quad (3)$$

Fig. 21 compares the value of the critical speed improvement factor for the non-homogeneous soil cases and for the two area replacement ratios studied.

It can be observed how in the stiffest soil, the improvement brought about by the stone columns is less than in the case of the softest soil. In fact, VIF values for the softest soil range from 1.37 ( $a_r = 23\%$ ) to 1.52 ( $a_r = 33\%$ ), while for the stiffest soil the values are between 1.28 ( $a_r = 23\%$ ) and 1.39 ( $a_r = 33\%$ ). This indicates that the contrast in stiffness between the soil and that of the reinforcement material is an interesting parameter for evaluating the effectiveness of the stone columns. The greater the contrast, the bigger the improvement. Moreover, a higher  $a_r$  implies a greater increase in the critical speed. It can also be observed in Fig. 21 how  $a_r = 23\%$  has hardly any influence on the critical length.

With these results, it is clear that the most restrictive parameter for the dimensioning of the ground improvement in high-speed railway lines on soft soils is the critical speed. Moreover, at present, this is the major limitation on the speed of train operation for the railway administrations.

### Conclusions

This paper presents the first study of the critical length of stone columns supported ground in high-speed railway lines on soft soils. Three different scenarios have been proposed with respect to the

ground: one homogenous soil and two non-homogenous soils (normally dispersive and whose stiffness increases with depth). Also, two replacement rates have been considered for the stone columns. A systematic analysis has been made of the critical length according to three parameters which are all important in railway dynamics: maximum rail displacement, DAF and critical speed. The main conclusions are as follows:

- Regarding the rail displacement, DAF and critical speed, the most restrictive critical length value corresponds to the critical speed and the least restrictive to the DAF. The critical column length with respect to the maximum rail displacement is similar to that of the static case.
- It has been shown how, in the case of homogenous soils, the effect of the stone columns on the critical speed is insignificant, since it corresponds to an inversely dispersive case. The effects on the rail displacement and the DAF are substantial, reducing the rail displacement by a half. In these cases, an approach that focuses more on the mechanics of the track and the stress-strain state of the ground might be an alternative that could enable an increase in the speed of train operation in safe conditions.
- When the ground profile corresponds to a normally dispersive case, the effect of the stone columns is significant, considerably increasing the critical speed values and reducing the rail displacement and the DAF. Increases in the critical speed of between 28 and 52% have been obtained, which are quite substantial amounts. A higher replacement rate leads to a greater increase in the critical speed due to a greater stiffness in the reinforced ground. However, the area replacement ratio has a negligible influence on the critical length for the studied cases.
- The efficiency of the stone columns is greater the bigger the contrast in the stiffness between them and the ground. Hence, this soil improvement technique is more efficient for soft soils as already known for static loads.
- The critical length is reduced with an increase in the stiffness of the soil, since the critical speed phenomenon occurs at a higher frequency, thus reducing the wavelength and therefore the depth of influence. Moreover, when the stiffness of the soil increases it has been observed that the stress concentration ratio decreases, as does the critical length.
- The critical length with respect to the critical speed can be related to the dynamic pressure bulb length of the ground without reinforcement, giving a ratio of approximately 1.5. This rule cannot be generalised to other cases, but in cases of floating columns similar to the ones studied here, it may be a first order of magnitude in the early stages of design.

#### CRedit authorship contribution statement

**Jesús Fernández-Ruiz:** Conceptualization, Methodology, Writing - original draft, Investigation, Formal analysis, Visualization, Writing - review & editing. **Marina Miranda:** Conceptualization, Methodology, Writing - original draft, Investigation, Formal analysis, Writing - review & editing. **Jorge Castro:** Conceptualization, Supervision, Writing - review & editing, Resources. **Luis Medina Rodríguez:** Conceptualization, Supervision, Writing - review & editing.

#### Declaration of Competing Interest

The authors declare that they have no known competing financial interests or personal relationships that could have appeared to influence the work reported in this paper.

#### Appendix A. Supplementary material

Supplementary data to this article can be found online at <https://doi.org/10.1016/j.trgeo.2021.100628>.

[org/10.1016/j.trgeo.2021.100628](https://doi.org/10.1016/j.trgeo.2021.100628).

#### References

- [1] Abu Sayeed Md, Shahin MA. Three-dimensional numerical modelling of ballasted railway track foundations for high-speed trains with special reference to critical speed. *Transport. Geotech.* 2016;6:55–65. <https://doi.org/10.1016/j.trgeo.2016.01.003>.
- [2] Alves Costa P, Calçada R, Silva Cardoso A, Bodare A. Influence of soil non-linearity on the dynamic response of high-speed railway tracks. *Soil Dynam. Earthq. Eng.* 2010;30(4):221–35.
- [3] Alves Costa P, Calçada R, Silva Cardoso A. Track-ground vibrations induced by railway traffic: in-situ measurements and validation of a 2.5D FEM-BEM model. *Soil Dynam. Earthq. Eng.* 2012;30:111–28. <https://doi.org/10.1016/j.soildyn.2011.09.002>.
- [4] Alves Costa P, Colaço A, Calçada R, Cardoso AS. Critical speed of railway tracks. Detailed and simplified approaches. *Transport. Geotech.* 2015;2:30–46.
- [5] Alves Costa P, Lopes P, Silva Cardoso A. Soil shakedown analysis of slab railway tracks: numerical approach and parametric study. *Transport. Geotech.* 2018;16: 85–96.
- [6] Alves Costa P, Soares P, Colaço A, Lopes P, Connolly D. Railway critical speed assessment: A simple experimental-analytical approach. *Soil Dynam. Earthq. Eng.* 2020;134:106156. <https://doi.org/10.1016/j.soildyn.2020.106156>.
- [7] Babu MRD, Nayak S, Shivashankar R. A critical review of construction, analysis and behaviour of stone columns. *Geotech. Geol. Eng.* 2013;31:1–22.
- [8] Barksdale RT, Bachus RC. Design and construction of stone columns. Springfield: Nat Tech Information Service; 1983. Report FHWA/RD-83/026.
- [9] Brinkgreve RBJ, Kumarswamy S, Swolfs WM, Zampich L, Ragi Manoj N. *Plaxis 2019 User Manuals*. Delft: Plaxis bv; 2019.
- [10] Castro J. Numerical modelling of stone columns beneath a rigid footing. *Comput. Geotech.* 2014;60:77–87.
- [11] Castro J. Modeling Stone Columns. *Materials* 2017;10(7):782. <https://doi.org/10.3390/ma10070782>.
- [12] Castro J, Miranda M, Da Costa A, Cañizal J, Sagasetta C. Critical length of stone columns. *Proc. XVII ECSMG-2019 2019 Reykjavik*.
- [13] Chen J, Zhou Y. Dynamic responses of subgrade under double-line high-speed railway. *Soil Dynam. Earthq. Eng.* 2018;110:1–12. <https://doi.org/10.1016/j.soildyn.2018.03.028>.
- [14] Darendeli M. Development of a new family of normalized modulus reduction and material damping curves. PhD Dissertation. University of Texas at Austin; 2001.
- [15] Dieterman HA, Metrikine A. The equivalent stiffness of a half-space interacting with a beam. Critical velocities of a moving load along the beam. *Eur. J. Mech. A/Solids* 1996;15(1):67–90.
- [16] Dieterman HA, Metrikine A. Steady-state displacements of a beam on an elastic half-space due to a uniformly moving constant load. *Eur. J. Mech. A/Solids* 1997; 16(2):295–306.
- [17] Dong K, Connolly DP, Laghrouche O, Woodward PK, Alves Costa P. The stiffening of soft soils on railway lines. *Transport. Geotech.* 2018;17:178–91.
- [18] Dong K, Connolly DP, Laghrouche O, Woodward PK, Alves Costa P. Non-linear soil behaviour on high speed rail lines. *Comput. Geotech.* 2019;112:302–18. <https://doi.org/10.1016/j.compgeo.2019.03.028>.
- [19] El Kacimi A, Woodward PK, Laghrouche O, Medero G. Time domain 3D finite element modelling of train-induced vibration at high speed. *Comput. Struct.* 2013; 118:66–73. <https://doi.org/10.1016/j.compstruc.2012.07.011>.
- [20] Fernández Ruiz J, Medina Rodríguez L. Application of an advanced soil constitutive model to the study of railway vibrations in tunnels through 2D numerical models: a real case in Madrid (Spain). *J. Construct.* 2015;14(3):55–63. <https://doi.org/10.4067/S0718-915X2015000300007>.
- [21] Fernández Ruiz J, Alves Costa P, Calçada R, Medina Rodríguez LE, Colaço A. Study of ground vibrations induced by railway traffic in a 3D FEM model formulated in the time domain: experimental validation. *Struct. Infrastruct. Eng.* 2017;13(5): 652–64. <https://doi.org/10.1080/15732479.2016.1172649>.
- [22] Fernández Ruiz J, Soares PJ, Alves Costa P, Connolly DP. The effect of tunnel construction on future underground railway vibrations. *Soil Dynam. Earthq. Eng.* 2019;125:105756. <https://doi.org/10.1016/j.soildyn.2019.105756>.
- [23] Fernández-Ruiz J, Medina Rodríguez LE, Costa PA. Use of Tyre-Derived Aggregate as Backfill Material for Wave Barriers to Mitigate Railway-Induced Ground Vibrations. *Int. J. Environ. Res. Public Health.* 2020;17(24):9191. <https://doi.org/10.3390/ijerph17249191>.
- [24] Fernández-Ruiz J, Medina Rodríguez LE, Alves Costa P, Martínez-Díaz M. Benchmarking of two three-dimensional numerical models in time/space domain to predict railway-induced ground vibrations. *Earthq. Eng. Eng. Vib.* 2021;20: 245–56. <https://doi.org/10.1007/s11803-021-2017-8>.
- [25] Galavi V, Brinkgreve RBJ. Finite element modelling of geotechnical structures subjected to moving loads. In: Hicks et al., editors. VIII ECNUMGE – numerical methods in geotechnical engineering. Delft, Netherlands: Taylor & Francis – Balkema; 2014. Pp. 235–40.
- [26] Germonpré M, Degrande G, Lombaert G. Periodic track model for the prediction of railway induced vibration due to parametric excitation. *Transport. Geotech.* 2018; 17:88–108. <https://doi.org/10.1016/j.trgeo.2018.09.015>.
- [27] Hall L. Simulations and analyses of train-induced ground vibrations in finite element models. *Soil Dynam. Earthq. Eng.* 2003;23:403–13.
- [28] Han J. *Principles and Practice of Ground Improvement*. Hoboken. New Jersey: Wiley; 2015.

- [29] Hughes JMO, Withers NJ. Reinforcing of soft cohesive soils with stone columns. *Ground Eng.* 1974;7(3):42–9.
- [30] Karlstrom A, Bostrom B. An analytical model for train-induced ground vibrations from trains. *J. Sound. Vib.* 2006;292:221–41.
- [31] Kaynia M, Madshus C, Zackrisson P. Ground vibrations from high-speed trains: prediction and countermeasure. *J. Geotech. Geoenviron. Eng.* 2000;126(6):531–7.
- [32] Kece E, Reikalas V, DeBold R, Ho CL, Robertson I, Forde MC. Evaluating ground vibrations induced by high-speed trains. *Transport. Geotech.* 2019;20:100236. <https://doi.org/10.1016/j.trgeo.2019.03.004>.
- [33] Kirsch K, Kirsch F. *Ground improvement by deep vibratory methods*. London: Spon press; 2010.
- [34] Kouroussis G, Verlinden O, Conti C. Finite-dynamic model for infinite media: Corrected solution of viscous boundary efficiency. *J. Eng. Mech.* 2011;137(7): 509–11.
- [35] Krylov V. Generation of ground vibrations by superfast trains. *Appl. Acoust.* 1995; 44:149–64.
- [36] Lombaert G, Degrande G. Ground-borne vibration due to static and dynamic axle loads of InterCity and high-speed trains. *J Sound Vib* 2009;319:1036–66.
- [37] Lysmer J, Kuhlmeyer RL. Finite dynamic model for infinite media. *J. Eng. Mech.* 1969;95:859–77.
- [38] Madshus C, Kaynia M. High-speed railway lines on soft ground: dynamic behaviour at critical train speed. *J. Sound. Vib.* 2000;231(3):689–701.
- [39] Madshus C, Lacasse S, Kaynia A, Harvik L. Geodynamic challenges in high speed railway projects. In: *GeoTrans 2004 - geotechnical engineering for transportation projects*, ASCE; 2004. p. 192–215. Los Angeles.
- [40] Mezher SB, Connolly DP, Woodward PK, Laghrouche O, Pombo J, Alves Costa P. Railway critical velocity-Analytical prediction and analysis. *Transport. Geotech.* 2016;6:84–96.
- [41] Sheng X, Jones C, Thompson D. A theoretical study on the influence of the track on train-induced ground vibration. *J. Sound. Vib.* 2004;272:909–36.
- [42] Shih JY, Thompson DJ, Zervos A. The influence of soil nonlinear properties on the track/ground vibration induced by trains running on soft ground. *Transport. Geotech.* 2017;11:1–16. <https://doi.org/10.1016/j.trgeo.2017.03.001>.
- [43] Steenbergen MJMM, Metrikine AV, Esveld C. Assessment of design parameters of a slab track railway system from a dynamic viewpoint. *J. Sound. Vib.* 2007;306 (1–2):361–71.
- [44] Takemiya H. Simulation of track–ground vibrations due to a high-speed train: the case of X-2000 at Ledsgard. *J. Sound. Vib.* 2003;261:503–26.
- [45] Zhai W, He Z, Song X. Prediction of high-speed train induced ground vibration based on train-track-ground system model. *Earthq. Eng. Eng. Vibr.* 2010;9(4): 545–54.